Proceedings of ICFDP8:
Eighth International Congress of Fluid Dynamics & Propulsion
December 14-17, 2006, Sharm El-Shiekh, Sinai, Egypt

ICFDP8-EG-163

EXPERIMENTAL AND NUMERICAL STUDY OF AIR JET VORTEX GENERATOR FOR SUBSONIC FLOW

Paweł Flaszyński
Gdansk University of Technology,
Narutowicza11/12, PL-80 952 Gdansk, Poland

Ryszard Szwaba
IMP PAN
Fiszera 14, PL-80 952 Gdansk, Poland

Piotr Doerffer
IMP PAN
Fiszera 14, PL-80 952 Gdansk, Poland

ABSTRACT

The objective of the presented work is to perform an experimental and numerical study for single passive air jet vortex generator. Measurements have been done for Mach number 0.3 and 0.8 (main flow). Experimental data are compared with numerical results performed by means of low-Reynolds two-equations turbulence models with two codes: in-house code SPARC and Fluent. Comparison allows to assess numerical prediction of the streamwise vortex location and its intensity.

Optimization of the air jet vortex generator at the main flow Mach number 0.3 have been performed by means of genetic algorithm based on Fluent results. The maximum vorticity downstream of the jet hole is defined as a objective function of the two variables: jet skew and pitch angles.

INTRODUCTION

Streamwise vortices (SV) have been known already for a very long time to play an important role in flow control methods. Typical vortex generators (VG) are currently of the fixed type (vane type). Fixed type VG are preferred until now because of their reliability and maintenance free work. But already in the 70's it was shown that air-jet vortex generators (AJVG) are of the same effectiveness as fixed VGs even in supersonic flows. In the 90's the research on AJVG was continued in subsonic flow regime [1][2][3].

In the case of internal flows, as in gas turbines, many means of heat exchange enhancement devices are used. Very often an injection of coolant through holes and slots is applied in gas turbines. It is proposed here to take into account that the cooling jets may be used for the flow control as well. Enhancement of mixing and simultaneous introduction of flow control may be reached by applying jets as streamwise vortex generators. Application of AJVG in turbomachinery needs very careful consideration because the flow structure in these machines is three-dimensional and very complex.

In order to approach these problems the authors [4] investigated the interaction of chosen elements of the three dimensional flow with a single streamwise vortex at the beginning. The most typical element of vortical 3-D structure, not only in turbomachinery, is the horseshoe vortex (HSV). It is generated by every leading edge being embedded in the boundary layer. In order to generate the horseshoe vortex a symmetric profile was used. Its leading edge curvature and the following thickness increase were designed basing on a real NGV profile. The inlet boundary layer thickness has been chosen in proportion to these dimensions. This way the horseshoe vortex formation was similar to real gas turbine configuration.

The effect of the SV on the horseshoe vortex is strongly dependent on the AJVG location in relation to the blade leading edge. It should be mentioned that always the whole HSV structure is affected by a SV. However, when the AJVG is located just upstream of the blade leading edge one side of the HSV is nearly completely disintegrated. This interesting conclusion inspired present analysis of a streamwise vortex development on the more basic level without interaction with other vortex structures.

TEST SECTION AND MEASUREMENTS DESCRIPTION

A view of the test stand and the main measurement sections is shown in Fig. 1. Lower and upper wall of the nozzle is flat. It facilitates the possibility to obtain the constant flow velocity both upstream and downstream the jet hole. The inclination of the upper wall is adjustable. It allows to compensate the increase of the boundary layer thickness on the all nozzle walls and finally to obtain a constant velocity in the measurement section.

The analyzed AJVG is a passive type. The main flow and jet inlet stagnation parameters are similar. The only difference arises from losses in the inlet ducts.

In Fig. 1, the static pressure measurement taps are also shown. The 9 taps are located on the lower wall upstream of the measurement plate. They are spaced every 50 mm, the first tap is located 420 m upstream of the plate.

The more detailed view of the measurement plate and its measurement regions are shown in Fig. 2. Nine vortex generators are drilled in the plate using: three different

diameters (0.5, 1 and 2 mm) and three different pitch angles (*theta*): 30º, 45º and 60º (inclination to XY plane). The skew angle (*alfa*) 90° (in XY plane) is the same for all holes of the vortex generator plate. The measurement results presented in this paper concern only vortex generated by the hole of 1 mm diameter, pitch angle *theta* 45° (in YZ plane) and as mentioned skew angle (*alfa*) 90°.

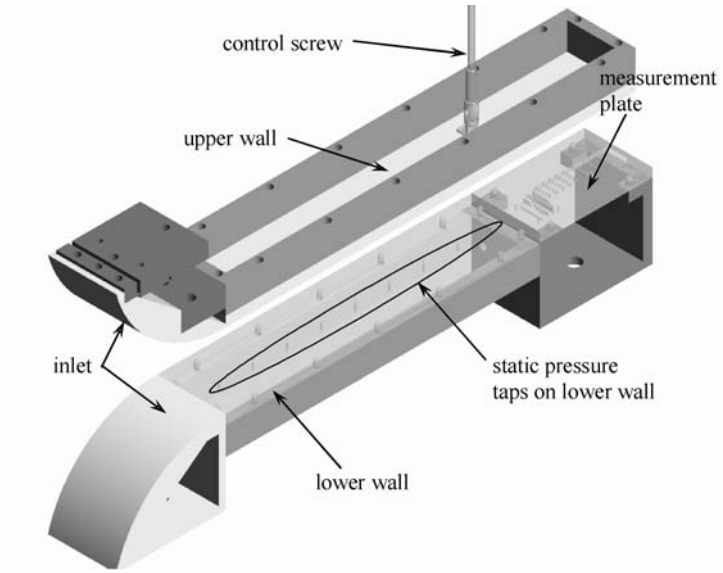

Fig. 1 General view of the nozzle

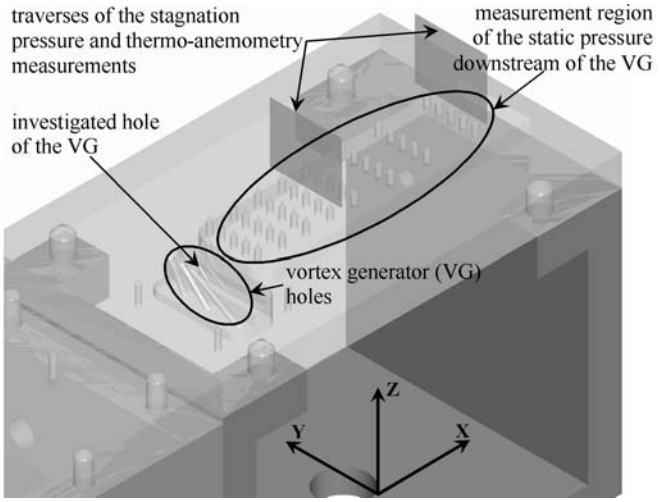

Fig. 2 View of the measurement plate

The location of this hole is shown in Fig. 2. The pressure measurement taps are located downstream of the vortex generator. These taps are manufactured in 5 columns and 8 rows. At the two traversing planes, 48 and 108 mm downstream of the VG hole (Fig. 2), the total pressure measurements were carried out. The total pressure is measured with Pitot probe of the 0.5 mm outer diameter. The transport of the probe and the data acquisition were controlled by the computer system. Mass flow in the jet hole is measured with the laminar flowmeter.

NUMERICAL MODEL DESCRIPTION

Numerical analysis have been performed by means of two codes, SPARC (Structured Parallel Research Code) [5] and Fluent 6.2. Both of them are based on finite volume method. Central difference approximation is used for convection terms in SPARC where the scheme is stabilized by artificial dissipation model introduced by Swanson-Turkel [6] and Martinelli-Jameson [7]. In case of Fluent simulation, the second order upwind scheme is applied for the convection terms.

Geometry of the computational domain (Fig.3) is defined in accordance with the test section geometry. The computations were performed on the structured mesh generated with IGG-Numeca (Interactive Grid Generator). The mesh consists of 1,793,280 cells and it is refined close to walls in order to keep $y^+ \approx 1$.

Numerical simulations were done on the identical mesh in case of both codes: SPARC and Fluent. They differ from each other by the turbulence models. In the case of SPARC, k-tau model in Craft-Launder-Suga formulation was used and in the Fluent case, k-omega SST model was selected.

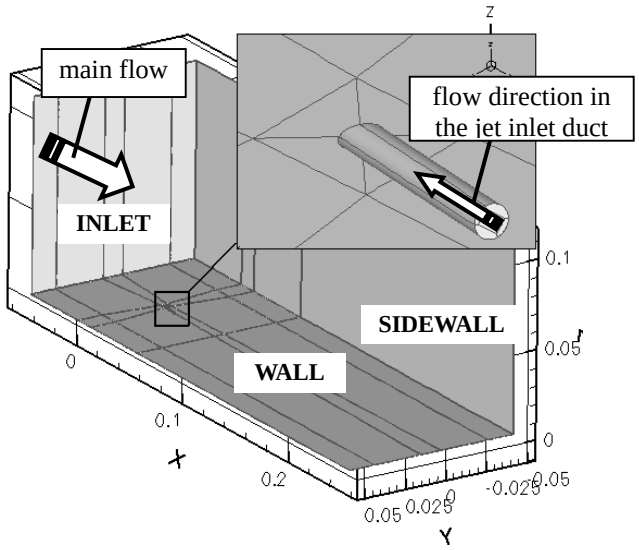

Fig.3 Computational domain (view from the outer side)

Boundary conditions were set accordingly to the measured data. At the main flow inlet (50 mm upstream of the AJVG hole) boundary layer profile is prescribed. Unfortunately, it is not possible to set boundary conditions in the same way in both codes. Velocity profile is set in SPARC but in Fluent the same boundary layer distribution is defined by the total pressure. Nevertheless, in both cases boundary layer thickness is equal to 12 mm (according to measurements) and the profile is approximated by the 1/7 power law profile very well. Total temperature is equal to 283 K at the inlet. The turbulence intensity and turbulent viscosity ratio are set to 1% and 10

respectively. At the outlet plane, static pressure is set to obtain required Mach number 0.3 and 0.8. At the hole inlet (jet), two approaches were applied depending on the code boundary conditions options. For Fluent code mass flow inlet boundary condition is used based on the measured values 6.554ÿ10^{-5} kg/s (Ma=0.3) and 14.25ÿ10^{-5} kg/s (Ma=0.8). In SPARC, due to the lack of mass flow boundary condition it is necessary to adjust the total pressure at the inlet in order to obtain required mass flow. The simulations have been performed for a steady state by the ideal gas assumption and with Sutherland formula for viscosity

COMPARISON OF EXPERIMENTAL DATA AND NUMERICAL RESULTS

The first important point of numerical results and experimental data comparison is boundary layer profile and its evolution. As it was mention, the boundary layer profile is set as a boundary conditions 50mm upstream the hole (jet outlet). The next control sections are located 48 and 108mm downstream to hole. In Fig. 4 and 5, the comparison of the total pressure profile for Mach number 0.3 is presented. The compared profiles concern the flow area not influenced by the jet. One can notice that both codes underestimate shear stresses at the wall in spite of "agreement" at the inlet boundary conditions plane. The slight deviation of the profile is very similar in SPARC and Fluent case, although boundary layer thickness remains the same.

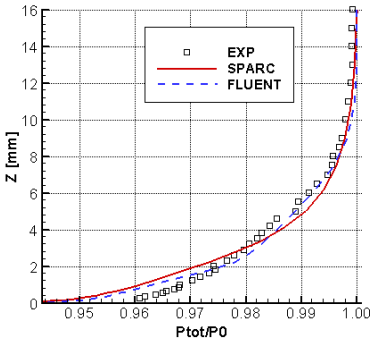

Fig.4 Boundary layer 48 mm downstream of the hole (Ma = 0.3)

In the case of Mach number 0.8, the differences look very similar to the previous ones. Fluent results give a bit less deviation to experimental data than SPARC especially as far as wall shear is concerned.

Boundary layer distribution of the measured total pressure in the area of jet influence is presented in Fig. 6 and Fig. 7. The color map refers to the total pressure normalized at each height (z=const) by the total pressure value undisturbed by the jet at this height $\tilde{p}$. The streamwise vortex direction of rotation is marked by the arrow. The jet inclination is marked by the straight arrow in both figures. The bright colour indicates the higher local total pressure value than in the undisturbed flow. It means momentum transport from the outer zone of boundary layer to the layer close to wall. The dark colour range is related to the low momentum boundary layer zone which is lifted off locally.

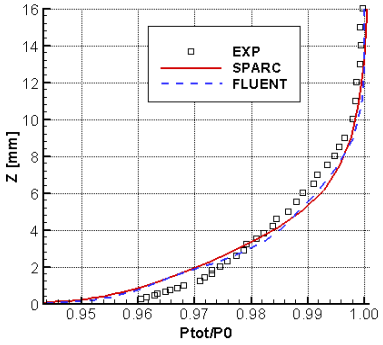

Fig.5 Boundary layer 108 mm downstream of the hole (Ma = 0.3)

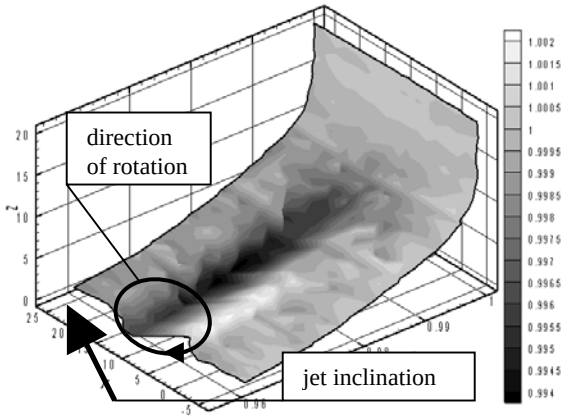

Fig.6 Boundary layer $\tilde{p}$ (exp) 108 mm downstream to hole (Ma = 0.3)

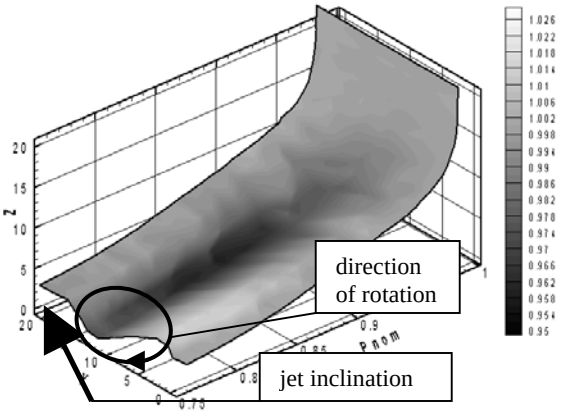

Fig.7 Boundary layer $\tilde{p}$ (exp) 108 mm downstream to hole (Ma = 0.8)

Normalized total pressure $\tilde{p}$ can also be presented in plane view as it is shown for measured data (Ma=0.3) at two control planes in Fig.8-9. The direction of rotation is marked by white circle. The total pressure distribution indicates of lowering streamwise vortex intensity and increasing of influenced area

by the vortex. The jet location is marked by black arrow (y=7.5mm). Similar contour plots were performed for numerical results (Fig.10-13). In case of both codes, the results are in qualitatively good agreement with experimental data. However, quantitative differences are clearly visible and strongly depends on the code. Streamwise vortex predicted by SPARC is weaker than measured one and it is located higher than in the experiment and in Fluent code. The total pressure distribution obtained by means of Fluent relates to more concentrated vortex and stronger than the predicted by SPARC and even stronger than the measured one.

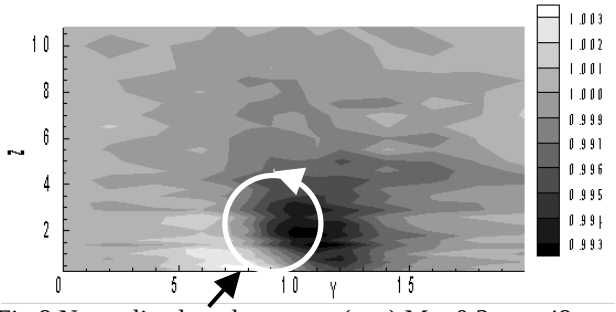

Fig.8 Normalized total pressure (exp) Ma=0.3; x = 48 mm

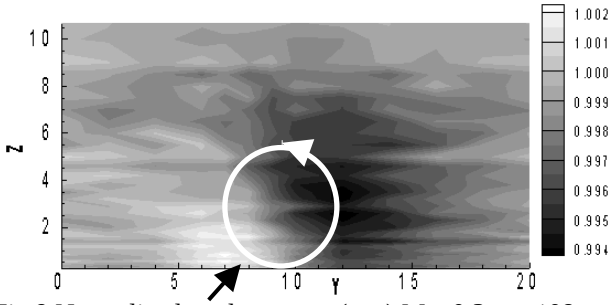

Fig.9 Normalized total pressure (exp) Ma=0.3; x= 108 mm

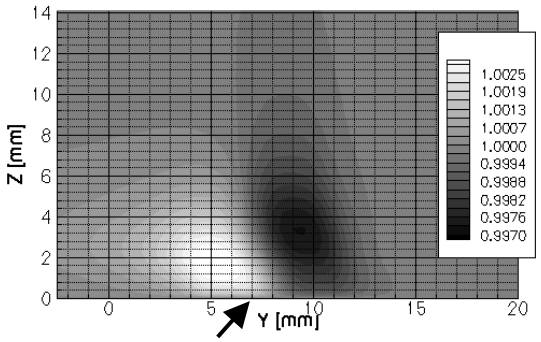

Fig.10 Normalized total pressure (SPARC) Ma=0.3; x = 48 mm

The very similar results are obtained at Mach number 0.8. The quality of measurements (Figs 14 and 15) seems to be better because the jet effect is stronger at higher velocity. In this case the intensity of the measured vortex is also higher than predicted by SPARC and lower then in Fluent simulations.

At the Mach number 0.8 the streamwise vortex is stronger than at Mach equal to 0.3 but its location referring to the jet hole is very similar.

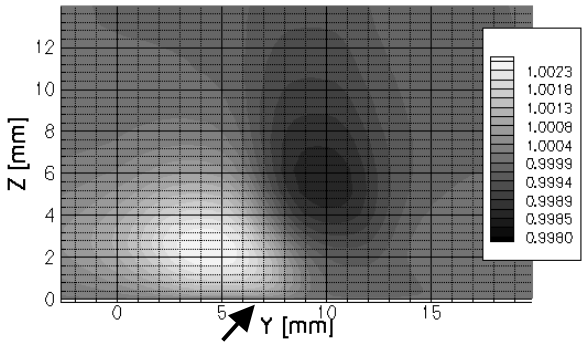

Fig.11 Normalized total pressure (SPARC) Ma=0.3; x= 108 mm

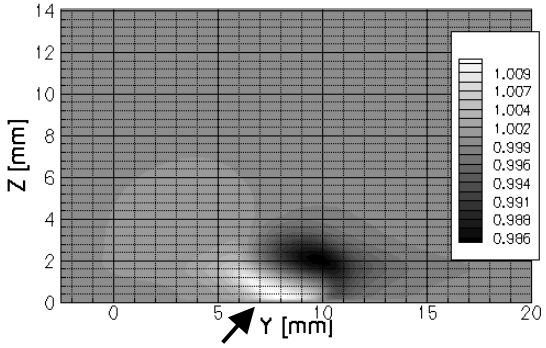

Fig.12 Normalized total pressure (Fluent) Ma=0.3; x = 48 mm

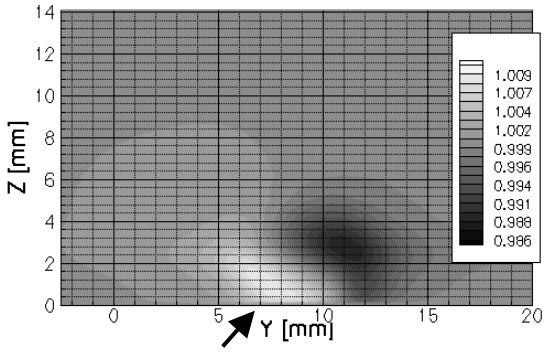

Fig.13 Normalized total pressure (Fluent) Ma=0.3; x = 108 mm

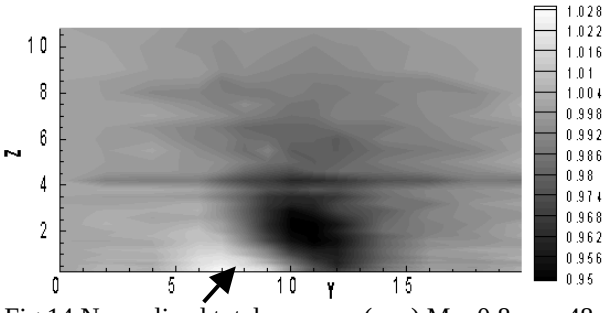

Fig.14 Normalized total pressure (exp) Ma=0.8; x = 48 mm

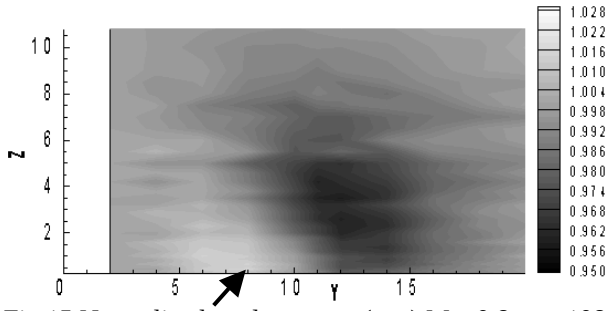

Fig.15 Normalized total pressure (exp) Ma=0.8; x = 108 mm

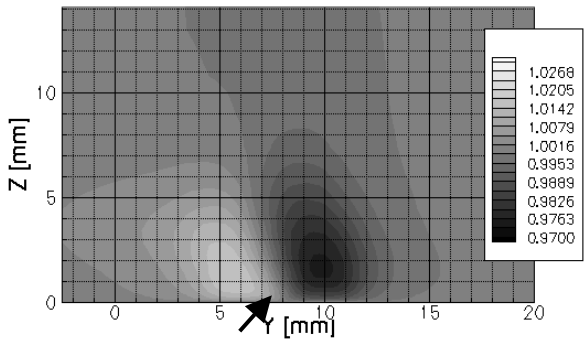

Fig.16 Normalized total pressure (SPARC) Ma=0.8; x = 48 mm

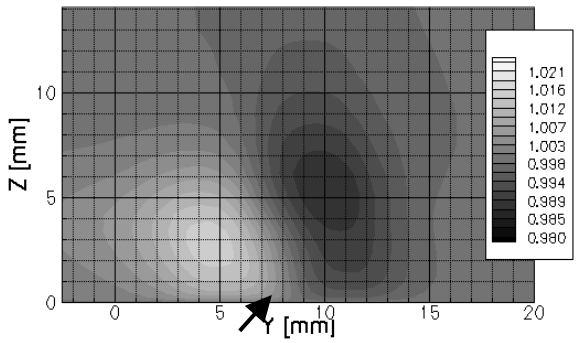

Fig.17 Normalized total pressure (SPARC) Ma=0.8; x= 108 mm

AIR JET VORTEX GENERATOR OPTIMISATION FOR MACH NUMBER 0.3

Comparison of numerical results and experimental data presented in the previous paragraph concerns one air jet vortex generator configuration, skew *alfa* (90**±**) and pitch *theta* (45**±**) angle. Application of the air jet vortex generator to flow control requires a selection of appropriate hole geometric configuration dependent on the flow case.

Optimization of the air jet vortex generator at the main flow Mach number 0.3 have been performed by means of genetic algorithm based on Fluent results for the geometry and boundary conditions presented in the previous paragraph. The side and upper wall boundary conditions were modified to symmetry (slip at the surfaces) in order to use coarser mesh far from the streamwise vortex influence. The mesh used in optimization consists of 870912 hexahedral. Computations have been launched on SGI Altix 3700 machine with 16 x Itanium2 (1.5GHz) devoted to this case.

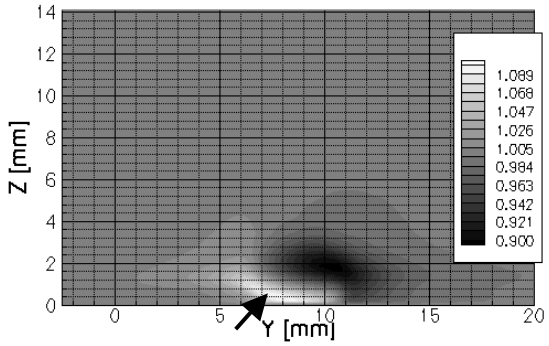

Fig.18 Normalized total pressure (Fluent) Ma=0.8; x = 48 mm

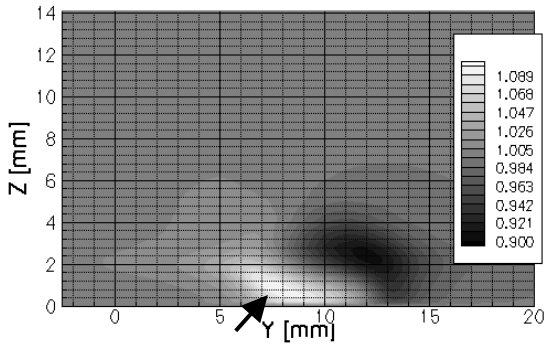

Fig.19 Normalized total pressure (Fluent) Ma=0.8; x = 108 mm

Maximum of vorticity X component at the section 50 mm (50 jet hole diameters) downstream of the jet hole is the objective function. The two variables have been chosen: jet skew angle *alfa* <30**±**,90**±**> and jet pitch angle *theta* <20**±**,90**±**>. The jet hole length is equal in the all cases.

Individuals representing the maximum x-vorticity as a function of jet skew angle and jet pitch angle are shown in Fig.20 and Fig.21, respectively. The generated vorticity is highly dependent on the combination of these two angles. The global extremum was found for *alfa* 58**±** and *thet*a 20**±**. Nevertheless, it is clearly visible the optimum of x-vorticity for the skew angle 60**±≤**5**±**. In the case of jet pitch angle, the maximum x-vorticity was found in the range of lower *theta* angles. The extremum was found for the minimum analyzed *theta* angle, but one can conclude that the optimal jet pitch angle for such formulated problem is in range <20**±**,35**±**> and this is a technical limit of the AJVG geometry.

The decay of maximum x-vorticity along the distance from the jet hole is shown for different cases of the obtained database in Fig.22 and Fig.23. The optimum configuration (*alfa* 58**±**, *thet*a 20**±**) is compared to some selected cases. It is shown that the maximum x-vorticity distribution along the streamwise vortex is similar in all cases and decays rapidly on a distance of 20-30 jet hole diameters.

CONCLUSIONS

The presented measurements of total pressure at two control sections downstream the jet hole allow to compare numerical results and to make quantitative assessment. Numerical analysis have been performed by means of two codes: SPARC and Fluent with low-Reynolds turbulence models approach. In case of both Mach numbers 0.3 and 0.8, the generated streamwise vortex is stronger (higher vorticity) for Fluent than for SPARC. The experimental data indicate lower vortex intensity prediction by SPARC than measured and stronger effect are predicted by Fluent.

Optimization of the air jet vortex generator for the main flow Mach number 0.3 by means of genetic algorithm have been performed. Results indicate of maximum vorticity existence for the jet skew angle 60±≤5± and the jet pitch angle in range <20±,35±>

ACKNOWLEDGMENTS

The presented results are obtained within a framework of the project granted by Polish Ministry of Scientific Research and Information Technology (MNI 3TB10 078 26).

Authors would like to thank TASK Academic Computer Centre for making computational resources available.

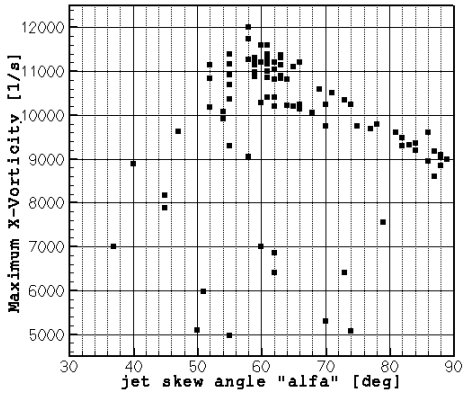

Fig.20 Maximum x-vorticity 50 mm downstream of jet hole

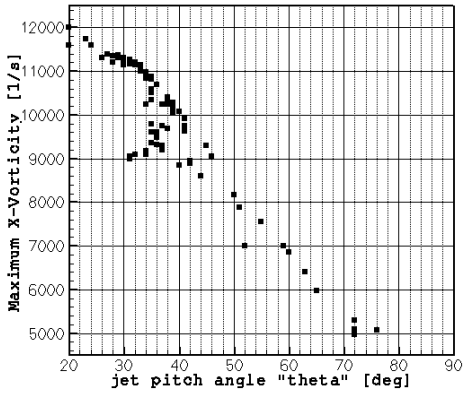

Fig.21 Maximum x-vorticity 50 mm downstream of jet hole

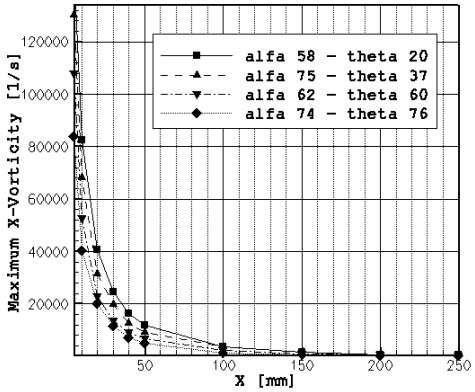

Fig.22 Decay of maximum x-vorticity along the distance to the jet hole

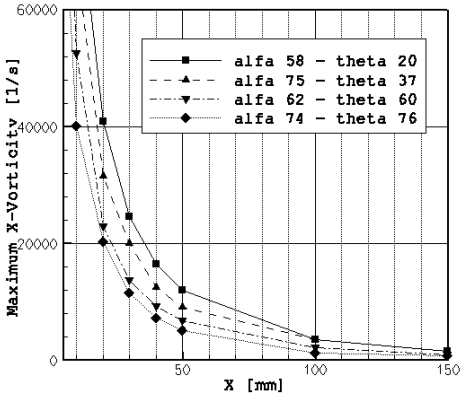

Fig.23 Modified range of Fig.22

REFERENCES

[1] Compton D.A., Johnston J.P.: Streamwise Vortex Production by pitched and Skewed Jets in a Turbulent Boundary Layer. AIAA Journal, March 1992, vol. 30, no. 3

[2] Johnston J.P, Mosier B.P., Khan Z.U.: Vortex Generating Jets, Effect of Jet-Hole Inlet Geometry. International Journal of Heat and Fluid Flow, 2002, vol. 23

[3] Kupper Ch., Henry F.S.: Numerical Study of Air-Jet Vortex Generators in a Turbulent Boundary Layer. Applied Mathematical Modelling, 2003, vol. 27

[4] Doerffer P., Flaszynski P., Magagnato F.: Streamwise Vortex Interaction with a Horseshoe Vortex. Journal of Thermal. Science, 2003, vol. 12 no. 4

[5] Magagnato F. : SPARC - Structured Parallel Research Code, TASK Quarterly, Vol. 2, No. 2, 1998, pp. 215 – 270

[6] Swanson R. C., Turkel E. : Artificial dissipation and central difference schemes for the Euler and NS-equations, AIAA-paper 87-1107, 1987

[7] Martinelli L., Jameson A. : Validation of a multigrid method for the Reynolds averaged equations, AIAA-paper 88-0411